Available online at www.sciencedirect.com
SCIENCE DIRECT
Polymer 47 (2006) 1132–1140
polymer
www.elsevier.com/locate/polymer

Multiwalled carbon nanotubes and nanofibers grafted with polyetherketones in mild and viscous polymeric acid

Se-Jin Oh [a], Hwa-Jeong Lee [a], Dong-Ki Keum [a], Seong-Woo Lee [b], David H. Wang [c], Soo-Young Park [b], Loon-Seng Tan [d,**], Jong-Beom Baek [a,*]

[a] School of Chemical Engineering, Chungbuk National University, Cheongju, Chungbuk 361-763, South Korea
[b] Department of Polymer Science, Kyungpook National University, Taegu 702-701, South Korea
[c] University of Dayton Research Institute, 300 College Park, Dayton, OH 45469, USA
[d] Polymer Branch, Materials and Manufacturing Directorate, AFRL/MLBP, Air Force Research Laboratory, Wright-Patterson Air Force Base, Dayton, OH 45433, USA

Received 28 October 2005; received in revised form 11 December 2005; accepted 19 December 2005
Available online 10 January 2006

Abstract

Direct covalent attachment of amorphous and semicrystalline polyetherketones onto the surface of either an as-received multi-walled carbon nanotube (MWNT) or a vapor-grown carbon nanofiber (VGCNF) in polyphosphoric acid (PPA) with optimized P_2O_5 content resulted in uniform grafting of polyetherketones to these carbon nanoscale materials. Soxhlet extraction experiment, the spectra from FT-IR spectroscopy and the clear images from high-resolution transmission electron microscopy showed that the covalent attachment is effective in uniformly coating the PEK grafts on the surfaces of both MWNT and VGCNF. Additionally, a drastic increase in solution viscosity due to the formation of giant molecules was monitored during polymerization. As such, the resulting nanocomposites were easily fabricated via a simple compression molding technique. The alignment possibility of MWNT and VGCNF grafted with semicrystalline PEK in these thermoplastic nanocomposites via solution fiber spinning was also demonstrated.

Keywords: Carbon nanotubes; Carbon nanofibers; Nanocomposites

1. Introduction

One-dimensional, nanoscale carbon-based materials are generally divided into three categories according to the number of walls and their diameter dimensions: (i) single-wall carbon nanotubes or SWNTs (0.7–3 nm); (ii) multi-wall carbon nanotubes or MWNTs (2–20 nm); (iii) carbon nanofibers or CNFs (40–100 nm) [1,2]. Although the unique properties of carbon nanotubes (CNTs) have been well known [3,4], there are two major issues related to the aspect ratio and interfacial adhesion when using CNT or CNF as a reinforcing additive and expecting enhanced properties from the resultant nanocomposites [5–12]. CNTs, especially single-walled carbon nanotubes, usually exist as ropes and bundles due to strong lateral interactions between the tubes, causing difficulty in homogeneously dispersing them in a multi-component system. As a result, their outstanding properties emerging from nanoscale could not be effectively transferred to matrix materials. To resolve this problem, various physical, chemical, or combined approaches have been reported to afford homogeneous dispersion of CNT in polymer solution or melt [13,14].

However, trying to have homogeneous dispersion in strong acidic media such as sulfuric acid and nitric acid make CNT into amorphous carbon materials [15,16]. Aided by a physical method such as sonication tends to accelerate imparting structural damages to CNT with respect to the exposure time and power level [17]. Furthermore, another concern is that the desired material properties of a nanocomposite invariably depend on the strength of specific interactions between CNT and matrix polymers. Mechanical properties of CNT nanocomposite via physical mixing, which are yet to approach the theoretical limits, would greatly depend on the homogeneity of CNT and strong interfacial interactions. Thus, noncovalent interactions between CNT and matrix in nanocomposite are not expected to have any synergic effect even after homogeneous

* Corresponding authors. Tel.: +82 43 261 2489; fax: +82 43 262 2380.
** Tel.: +1 937 255 9141; fax: +1 937 255 9157.
E-mail addresses: loon-seng.tan@wpafb.af.mil (L.-S. Tan), jbbaek@chungbuk.ac.kr (J.-B. Baek).

0032-3861/$ - see front matter © 2005 Elsevier Ltd. All rights reserved.
doi:10.1016/j.polymer.2005.12.064

CNT dispersion could be achieved. Introducing suitable chemical groups to the surface of CNT by chemical methods are more viable because they can better prevent close lateral contacts among the nanotubes, enabling higher degree of exfoliation and allowing better compatibility with matrix component [18–23]. CNTs, however, are generally inert and chemically resistant. A common approach to covalent modification of CNT requires harsh reaction conditions in strong acids such as sulfuric acid, nitric acid, etc. and/or their mixtures at elevated temperatures. Significant damages to the molecular framework of CNT are inevitable [15,16].

We developed an improved electrophilic substitution process to prepare high molecular weight polyetherketones in commercial polyphosphoric acid (PPA, 83% assay) with additional phosphorous pentoxide (P_2O_5) as a dehydrating agent to promote the Friedel–Crafts reaction efficiently [24]. We also demonstrated the functionalization of electron deficient vapor-grown carbon nanofiber (VGCNF) [25] and grafting of *meta*-polyetherketone or *m*PEK onto VGCNF by an in situ Friedel–Crafts polymerization of an AB monomer, 3-phenoxybenzoic acid, in the same medium [26]. Because of viscous character of PPA medium, prepared polymers displayed unusual thermal relaxation of viscosity-and-shear-induced strain [27]. We expect that PPA is a mild and less-destructive reaction medium and plays two important roles for the effective and thus uniform covalent attachment on the surface of carbon nanomaterials. The one is its moderate acidic nature promotes deaggregation to help homogeneous dispersion without damaging CNT and the other is viscous character helps to impede reaggregation after dispersion, which is achieved by shear force. In this paper, we describe our continuous effort on the grafting of *m*PEK and *para*-polyetherketone (*p*PEK) onto multi-walled carbon nanotube (MWNT) by in situ polycondensation of the AB monomers, 3- and 4-phenoxybenzoic acids in viscous PPA medium. For comparison purpose, VGCNF was also grafted with *m*PEK [26] and *p*PEK.

2. Experimental

2.1. Materials

All reagents and solvents were purchased from Aldrich Chemical Inc. and used as received, unless otherwise mentioned. The monomers, 3-phenoxybenzoic acid (3-PBA) and 4-phenoxybenzoic acid (4-PBA), were purified by recrystallization from toluene/heptane. Multi-walled carbon nanotube (MWNT, CVD MWNT 95) was obtained from Iljin Nanotech Co., Ltd, Seoul, Korea [28]. Vapor-grown carbon nanofiber (VGCNF, PR-19-HT) was obtained from Applied Sciences Inc., Cedarville, OH [29].

2.2. Instrumentation

Infrared (FT-IR) and Raman spectra were recorded on a Bruker Fourier-transform spectrophotometer IFS-66/FRA106S. Elemental analysis was performed with a CE Instruments EA1110. The melting points (m.p.) of all the compounds were determined on a Mel-Temp apparatus and are uncorrected. Differential scanning calorimetry (DSC) was performed under the nitrogen atmosphere with heating and cooling rates of 10 °C/min using a TA instrument model MDSC2910. The T_g's were taken from maximum inflections in baselines of the DSC traces. Thermogravimetric analysis (TGA) was conducted in nitrogen and air atmospheres with a heating rate of 10 °C/min using a TA instrument SDT 2960 thermogravimetric analyzer. The transmission electron microscope (TEM) employed in this work was a Philips CM-200 TEM with a LaB6 filament operating at 200 kV. For TEM, samples were dissolved in methanesulfonic acid (MSA) and diluted with *N*-methyl-2-pyrrolidinone (NMP). The samples were mounted on 200 mesh copper grids by dipping into the dilute solution and solvent was evaporated under reduced pressure (1 mm Hg). The field emission scanning electron microscopy (Zeiss-FESEM) used in this work was LEO 1530FE. For SEM, there was no specific treatment and all as-prepared nanocomposite samples with proper work-up procedure as described were mounted on conducting tape.

2.3. Representative procedure for in situ polymerization (AB monomer with 10 wt% MWNT Load)

Into a 250 mL resin flask equipped with a high torque mechanical stirrer, nitrogen inlet and outlet, and a solid-addition port, 4-phenoxybenzoic acid (5.4 g, 25.21 mmol), and MWNT (0.6 g), P_2O_5 (15.0 g) and PPA (83% P_2O_5 assay; 100 g) were placed and stirred under dry nitrogen purge at 130 °C for 48 h. The initially dark mixture due to dispersion of MWNT became more shiny and viscous as the polymerization progressed. At the end of the reaction, the color of mixture was shiny and dark brown, and the dope was poured into distilled water to form long single fiber. The resulting fiber bundles were chopped, collected, and washed with diluted ammonium hydroxide, and then Soxhlet-extracted with water (3 days) and methanol (3 days), and finally dried over phosphorous pentoxide under reduced pressure (0.05 mm Hg) at 100 °C for 72 h to give the product in quantitative yield. Anal. Calcd for $C_{14.98}H_8O_2$: C, 81.78%; H, 3.67%. Found: C, 80.19%; H, 3.61%.

3. Results and discussion

3.1. Characterization of MWNT and VGCNF

The average diameter and length of the MWNT (CVD MWNT 95) were 10–20 nm and 10–50 μm, respectively, [28]. Those of VGCNF (PR-19-HT) were 60–200 nm and 50–100 μm, respectively, [29]. The purity (carbon content) of the as-received MWNT and VGCNF were assessed by elemental analysis (Table 1). Some researchers have often considered VGCNFs as multi-wall nanotubes because of their hollow and concentric cores with submicron diameters. It is noteworthy that the as-received MWNT and VGCNF, which are prepared by chemical vapor deposition process, contain

Table 1
The diameter, length, and elemental analysis data for MWNT and VGCNF

Sample	Diameter (nm)	Length (μm)	Elemental analysis		
				C (%)	H (%)
MWNT	10–20	10–50	Calcd	100.00	0.00
			Found	96.68	0.15
VGCNF	60–200	30–100	Calcd	100.00	0.00
			Found	98.97	1.10

a significant amount of hydrogen (0.15 and 1.10 wt%, respectively), presumably attributable to the sp^3 C–H and sp^2 C–H defects as hydrocarbons are used as the major component in the feedstock for their productions [30–34]. These defects would provide primary sites that are susceptible to the electrophilic substitution reaction. On the basis of the foregoing rationalization, we have recently reported for the first time that direct functionalization and grafting onto as-received VGCNF are very effective in PPA/P_2O_5 medium [25,26]. However, we believe there must be other type of chemical reaction (s) between CNT and acylium ion to uniformly functionalize entire CNT [35].

3.2. In situ polymerization of AB monomers with MWNT or VGCNF

We have selected poly(oxy-1,3-phenylenecarbonyl-1,4-phenylene, *m*PEK) and poly(oxy-1,4-phenylenecarbonyl-1,4-phenylene, *p*PEK) as the matrix polymers mainly because the AB-monomers, 3-phenoxybenzoic acid (**1**) and 4-phenoxybenzoic acid (**2**) are commercially available, high MW *m*PEK and *p*PEK can be synthesized from corresponding monomers in PPA with an optimized P_2O_5 content [24]. Thus, the in situ polycondensation of each AB monomer in the presence of dispersed MWNT or VGCNF for comparison were carried out with a fixed feed ratio (1/9) of MWNT/monomer or VGCNF/monomer for all runs as depicted in Fig. 1 and Table 2. The initial color of the all reaction mixtures was black because of the MWNT or VGCNF dispersion.

In the cases of MWNT-*g*-*m*PEK [36] and VGCNF-*g*-*m*PEK [37], the color of the reaction mixtures changed from black to shiny (indicative homogeneous dispersion), deep purple-brown, as the reaction progressed at the polymerization temperature. The dope stuck to the stirring rod 130 °C within

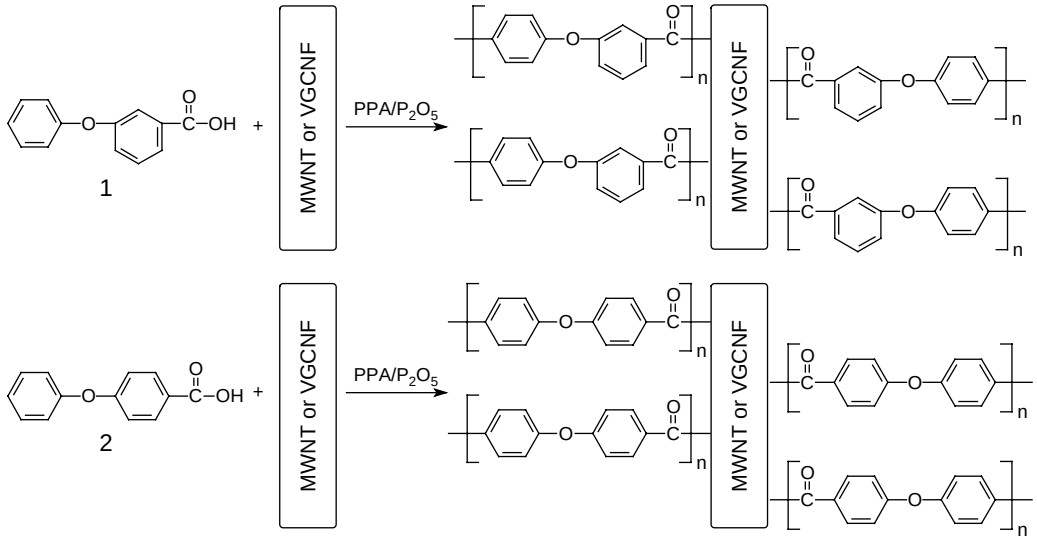

Fig. 1. In situ polymerization AB monomers with MWNT or VGCNF.

Table 2
Feed ratios of AB monomer and MWNT or VGCNF, thermogravimetric analysis and elemental analysis data

Feed ratio (wt/wt)		TGA in air		Elemental analysis		
10	90	Calcd	Found		C (%)	H (%)
MWNT	Monomer 1	10.8	11.0 at 600 °C	Calcd	81.78	3.67
				Found	80.00	3.61
MWNT	Monomer 2	10.8	ND[a]	Calcd	81.78	3.67
				Found	80.19	3.61
VGCNF	Monomer 1	10.8	11.1 at 675 °C	Calcd	81.78	3.67
				Found	80.28	3.68
VGCNF	Monomer 2	10.8	12.4 at 675 °C	Calcd	81.78	3.67
				Found	80.12	3.64

[a] ND, Not Detectable.

6 h, not allowing further efficient stirring and mixing via shearing the mixture against the vessel walls. However, this provided a visual signal that high MW polymer-grafted carbon nanocomposites were being synthesized and an indication to terminate reactions at the right time. The resulting dopes were quite elastic. Therefore, they could not be poured into water to spin fiber simply by force of gravity. Instead, water was added into the reaction vessel and big chunk of product was isolated in each case.

In the cases where *p*PEK was grafted to MWNT or VGCNF to afford MWNT-*g*-*p*PEK [38] or VGCNF-*g*-*p*PEK [39] in that order, the colors of the reaction mixtures were both shiny, deep dark-red. Due to the crystalline nature of *p*PEK, the viscosities of these dopes were visually not as high as those of MWNT-*g*-*m*PEK and MWNT-*g*-*m*VGCNF. The reaction mixtures were stirred at 130 °C for 48 h. Thus, the dopes could be poured into water to form long single fiber in each instance (Fig. 2(a) and (b)) [40,41], suggesting the possibility of aligning the MWNT and VGCNF in their nanocomposites via solution spinning to enhance the anisotropic tensile properties along the fiber axial direction [42–47]. Work is currently underway to optimize the CNT/CNF loading, lyotropic properties and fiber spinning conditions for these nanocomposites. The resultant nanocomposites were characterized by elemental analysis and thermogravimetric analysis (TGA). An excellent agreement is obtained for the weight percents of carbon and hydrogen between empirical and theoretical values for all samples (Table 2).

Fig. 2. Digital photographs of as-spun single fibers from (a) MWNT-*g*-*p*PEK and (b) VGCNF-*g*-*p*PEK in PPA/P_2O_5 dopes. Scales bars are 1 cm.

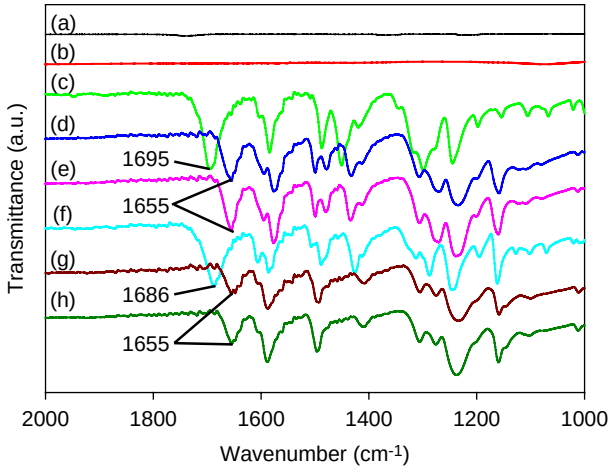

Fig. 3. FT-IR (KBr pellet) spectra of nanocomposites. (a) MWNT, (b) VGCNF, (c) 3-PBA, (d) MWNT-*g*-*m*PEK, (e) VGCNF-*g*-*m*PEK, (f) 4-PBA, (g) MWNT-*g*-*p*PEK, (h) VGCNF-*g*-*p*PEK.

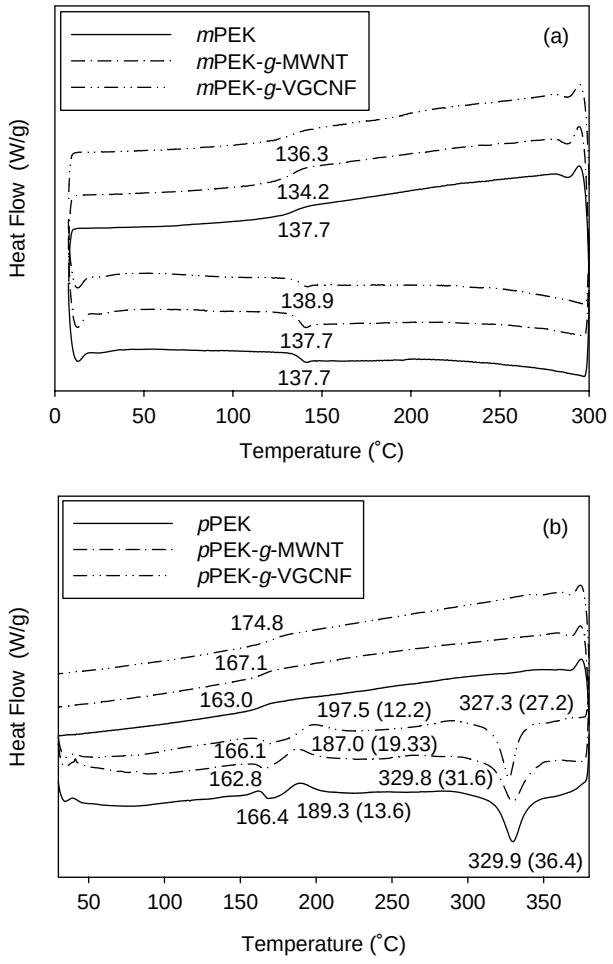

Fig. 4. DSC thermograms of PEK (solid), PEK-*g*-MWNT (dash–dot–dash) and PEK-*g*-VGCNF (dash–dot–dot–dash) samples run with heating and cooling rates of 10 °C/min: (a) *m*PEK; (b) *p*PEK.

3.3. FT-IR study

We have demonstrated that FT-IR spectrum of as-received VGCNF exhibits small sp^2 C–H and sp^3 C–H stretching bands at 2922 cm^{-1} that are attributable to the defects at sidewalls and open end of VGCNF [26]. The FT-IR spectrum of as-received MWNT also has similar stretching bands around 2969 cm^{-1} [48]. Logically, these defects would provide sites susceptible to the electrophilic substitution reaction. The covalent attachment of polymer to MWNT or VGCNF was conveniently monitored with FT-IR spectroscopy following the appearance of keto-carbonyl band at 1655 cm^{-1} associated with the product (Fig. 3). There were no keto-carbonyl bands, which are stemming from carboxylic acid moiety at the one end of polymer chain. This is indicative that one end of polymer are grafted to the surface of carbon nanomaterials. Furthermore, Soxhlet extractions of MWNT-*g*-*m*PEK and VGCNF-*g*-*m*PEK with dichloromethane, which is good solvent for *m*PEK, were carried out and there was only 2–3% weight loss for each case. In addition to this observation and our previous model study [25], we could assure that the covalent attachment of polymer chains to the carbon nanomaterials most probably occurred.

3.4. Thermal properties

The differential scanning caloriemetry (DSC) scans were run on the powder samples. The glass-transition temperatures (T_g's) of *m*PEK, MWNT-*g*-*m*PEK, and VGCNF-*g*-*m*PEK samples were determined by DSC and taken as the mid-point of the maximum baseline shift from the second run. As shown in Fig. 4(a), the pristine *m*PEK displayed a T_g at 137.7 and 137.7 °C from heating and cooling scans, respectively. Interestingly, MWNT-*g*-*m*PEK displayed the same T_g at 137.7 °C during heating scan and had a slightly lower T_g at 134.2 °C during cooling scan. VGCNF-*g*-*m*PEK displayed a T_g at 138.9 and 136.3 °C from heating and cooling scans, respectively. The values were similar to those of *m*PEK and MWNT-*g*-*m*PEK. Not like our previous results [26], all T_g's were of the same within experimental error, indicating that used carbon materials did not have significant effect on T_g's of *m*PEK's.

For the T_g's of *p*PEK, MWNT-*g*-*p*PEK and VGCNF-*g*-*p*PEK as shown in Fig. 4(b), the pristine *p*PEK displayed a T_g at 166.4 °C during heating scan and had 163.0 °C during cooling scan. MWNT-*g*-*p*PEK displayed a T_g at 162.8 and 161.1 °C from heating and cooling scans, respectively. VGCNF-*g*-*p*PEK

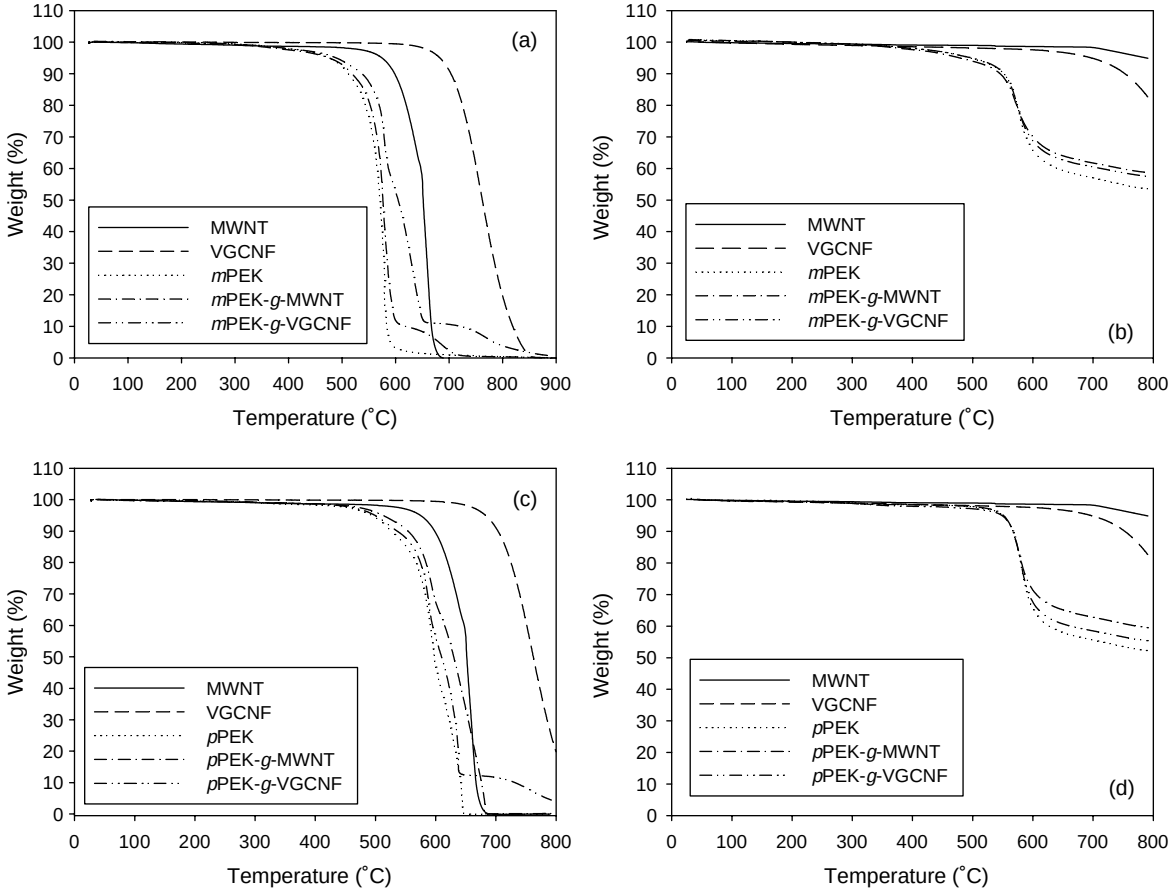

Fig. 5. TGA thermograms of MWNT (solid), VGCNF (medium-dash), PEK (dot), PEK-*g*-MWNT (dash–dot–dash), PEK-*g*-VGCNF (dash–dot–dot–dash) with heating rate of 20 °C/min: (a) in air; (b) in nitrogen; (c) in air; (d) in nitrogen.

displayed a T_g at 166.1 and 164.8 °C from heating and cooling scans, respectively. Interestingly, the PEK components, including the semicrystalline *p*PEK, in all samples remained amorphous during the polymer-forming process in such a viscous medium (PPA) and work-up stages. The relaxation exotherms of *p*PEK, MWNT-*g*-*p*PEK and VGCNF-*g*-*p*PEK appeared at 189.3, 187.0 and 197.5 °C, respectively. The exotherms interrupted the reading of T_g's on heating scan. Thus, the T_g's taken on cooling scan would give reliable number and comparison. In general, T_g increased when MWNT (10–20 nm) and VGCNF (60–200 nm) incorporated, and diameter increased from MWNT to VGCNF. The melting endotherm peaks were located in similar ranging 327–330 °C, but the heat of fusion (ΔH_f) decreased in the following order: *p*PEK > MWNT-*g*-*p*PEK–VGCNF-*g*-*p*PEK.

The thermogravimetric analysis (TGA) experiments on the powder samples of MWNT, VGCNF, *m*PEK, MWNT-*g*-*m*PEK and VGCNF-*g*-*m*PEK indicated that the temperatures at which a 5% weight loss ($T_{d5\%}$) in air occurred at 574, 683, 474, 478, and 489 °C in that order (Fig. 5(a)) and in nitrogen at 789, 697, 496, 479, and 496 °C in that order (Fig. 5(b)). VGCNF displayed the thermo-oxidative stability approximately 90 °C higher than that of MWNT (Table 2). The temperature difference in the thermo-oxidative stability between *m*PEK and MWNT in air was about 100 °C, which was large enough to discern the amount of residual char (11 wt%) attributable to MWNT at the on-set temperature 600 °C (Fig. 5(a)). This value agreed well with the calculated 10.8 wt% of MWNT in MWNT-*g*-*m*PEK. The temperature difference of thermo-oxidative stability between *m*PEK and VGCNF in air was approximately 210 °C to give residual VGCNF amount on plateau region at 675 °C to be 11%, which was in good agreement with the theoretical amount of VGCNF. In short, these consistencies provide the supporting evidence that MWNT and VGCNF were chemically intact during the polymerization in mild acidic and viscous reaction, and whole work-up procedures.

In the cases of *p*PEK, MWNT-*g*-*p*PEK and VGCNF-*g*-*p*PEK samples, the 5% weight loss ($T_{d5\%}$) in air occurred at 494, 513, and 499 °C in that order (Fig. 5(c)), and in nitrogen at 551, 552, and 550 °C in that order (Fig. 5(d)). The thermo-oxidative stability of *p*PEK in air was 20 °C higher than that of *m*PEK and 80 °C lower than that of MWNT. These values were too close to sort out the difference in the thermo-oxidative

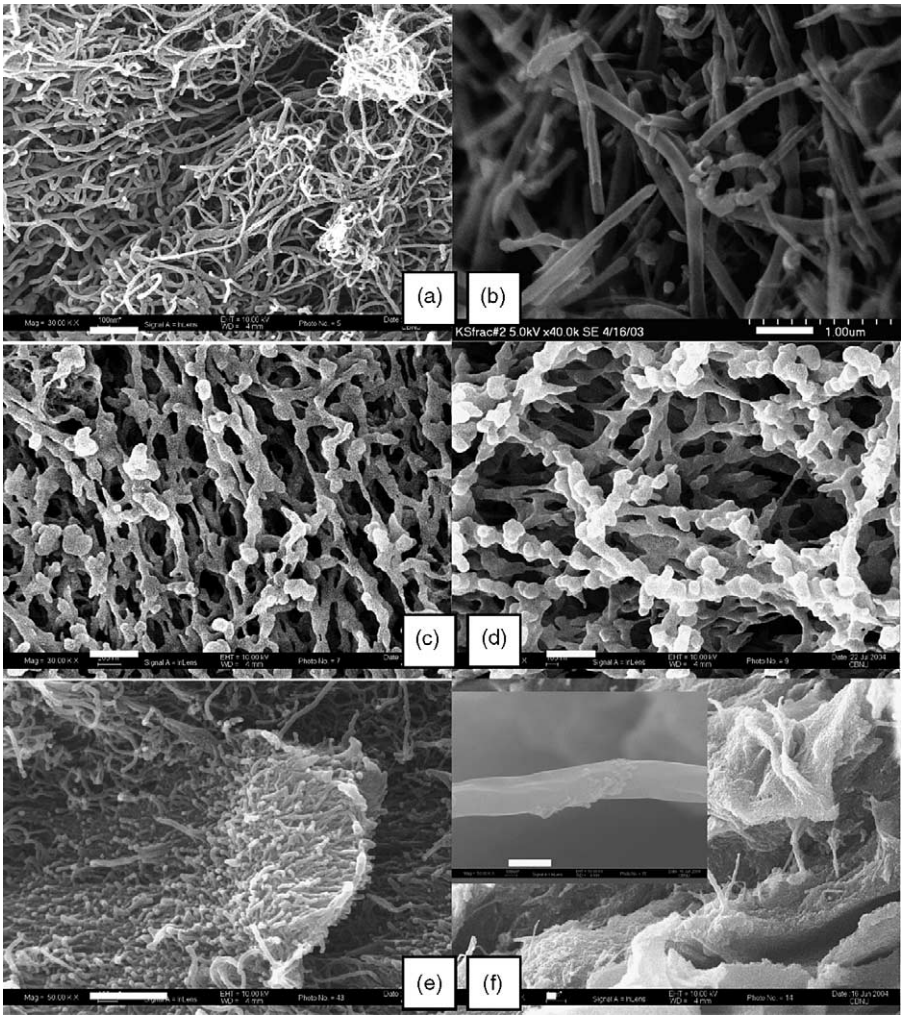

Fig. 6. SEM images (scale bar = 200 nm): (a) as-received MWNT (30,000×); (b) as-received VGCNF (40,000×); (c) MWNT-*g*-*m*PEK (30,000×); (d) VGCNF-*g*-*m*PEK (30,000×); (e) MWNT-*g*-*p*PEK (50,000×); (f) VGCNF-*g*-*p*PEK (5000×) and magnified SEM image (50,000×). Scale bars are 400 nm.

stability between MWNT and *p*PEK. Therefore, it is unclear whether MWNT has remained structurally intact based on TGA analysis. In contrast, after *p*PEK had been thermo-oxidatively stripped off from VGCNF-*g*-*p*PEK at 675 °C, 12.4 wt% of residual VGCNF remained versus 10.8 wt% expected (Table 2). All in all, the good agreement between the theoretical and experimental values for the *p*PEK/VGCNF compositions further lends support to our belief that the MWNT and VGCNF basically remained structurally intact during the in situ polymerization and the subsequent work-up.

3.5. Scanning electron microscopy (SEM)

The SEM images of pristine MWNT and VGCNF (Fig. 6(a) and (b), respectively) show that the tube surfaces are clean and smooth. However, the surfaces of MWNT-*g*-*m*PEK and VGCNF-*g*-*m*PEK (Fig. 6(c) and (d), respectively) are distinctly different in a side-by-side comparison with the unmodified MWNT and VGCNF. Both tube surfaces appear to be heavily and uniformly coated with *m*PEK, and thus clearly indicative of polymer grafting of MWNT and VGCNF. In the SEM images particularly viewed at the ends of polymer grafted MWNT and VGCNF (Fig. 6(c) and (d)) even clearly showed that the open ends of tubes (Fig. 6(b)) were heavily sealed with polymer shaping spherical ends (Fig. 6(d)). This may be due to larger population of sp^2C–H at the open ends of tubes, which could be more actively involved in the Friedel–Crafts acylation in PPA/P_2O_5 medium. The average diameters for both MWNT-*g*-*m*PEK and VGCNF-*g*-*m*PEK were increased by as much as 200 nm. This value was approximately equivalent to minimum 100 repeating units, assuming the polymer grafts were aligned vertically on the surfaces of MWNT or VGCNF and the length of each repeating unit is 1 nm. However, polymer chains are known to adopt several equilibrium chain conformations depending on the surface grafting density from random one to highly stretch one. Even in the condition of the highly stretched conformation, it is hard to obtain vertically aligned chains due to entropic loss. Thus, average change length is much longer than 100 repeating units, indicating that high molecular weight polymer chains are covalently attached to the carbon nanomaterials.

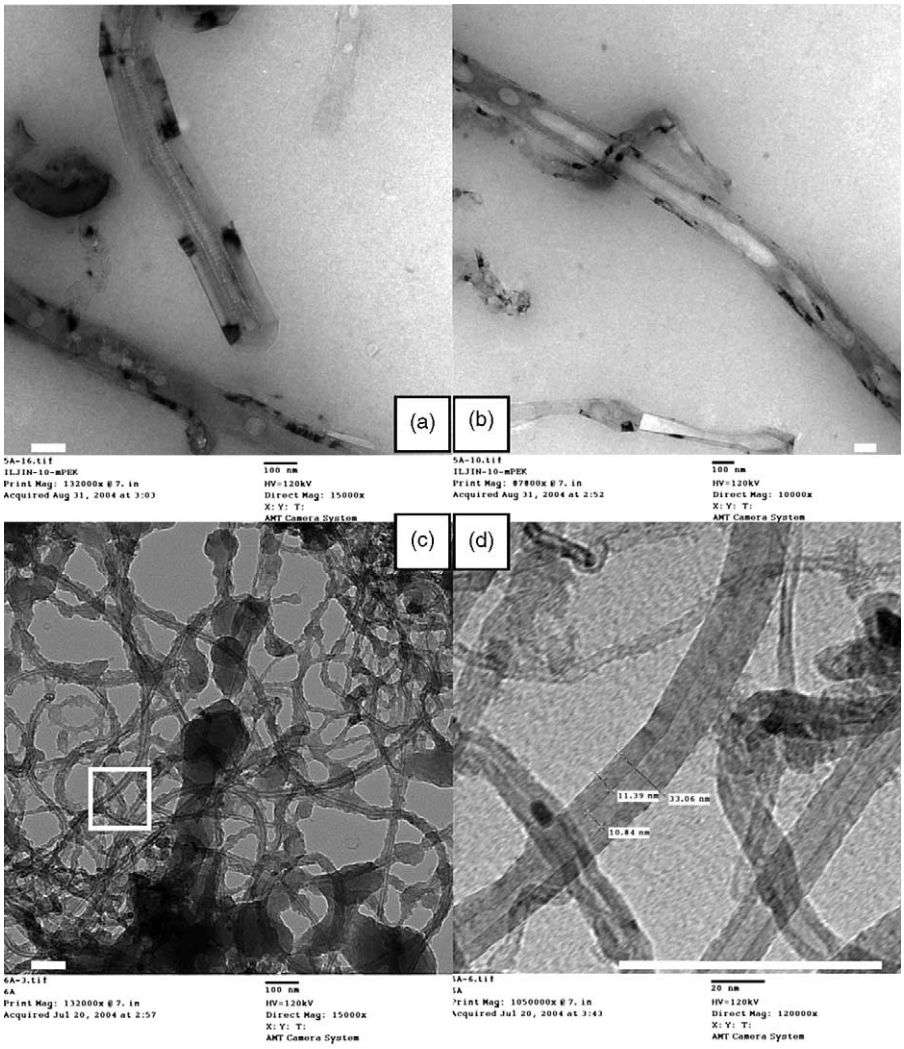

Fig. 7. TEM images obtained from (a) MWNT-*g*-*m*PEK; (b) VGCNF-*g*-*m*PEK; (c) MWNT-*g*-*p*PEK; (d) zoomed in the area of square at (c). Scale bars are 100 nm.

Similarly, SEM imaging showed that the surfaces of MWNT-*g*-*p*PEK and VGCNF-*g*-*p*PEK (Fig. 6(e) and (f), respectively) were also vastly transformed in comparison with the surfaces of the pristine MWNT and VGCNF (Fig. 6(a) and (b), respectively). The tube surfaces were heavily and uniformly decorated with *p*PEK moieties. The average diameters for both MWNT-*g*-*m*PEK and VGCNF-*g*-*m*PEK were also increased and the latter was as large as 400 nm (see the inset in Fig. 6(f)). This value was approximately equivalent to minimum 200 repeating units when the assumption the vertically aligned polymer chains attached on the surfaces of MWNT or VGCNF was applied.

3.6. Transmission electron microscopy (TEM) study

The TEM images of MWNT-*g*-*m*PEK (Fig. 7(a) and (b)) and MWNT-*g*-*p*PEK (Fig. 7(c) and (d)) showed that the MWNT remained structurally intact, again suggesting the stability of its nano-structural framework under the polymerization and work-up conditions. As clearly observed by TEM, polymers with thickness of 10–50 nm were uniformly grafted onto the surface of MWNT. The lower thickness compared to SEM observation could be stemming from the solvent-induced alignment of polymer chains to be parallel to the tube axis during sample preparation as described in experimental part. Thus, on the basis of the combined results from SEM and TEM studies, it could be reaffirmed that the electrophilic substitution reaction in PPA/P_2O_5 medium was indeed benign yet effective in covalently connecting an appropriate polymer onto the surfaces and open ends of electron deficient carbon nanotubes and nanofibers. On the basis of all supportive results, the reaction condition we developed is strong enough to be compatible with the electron-deficient handicap. Thus, efficient covalent modification onto CNT could be done very well.

However, the uniform covalent attachment of arylcarbonyl to electron-deficient CNT via electrophilic substitution reaction could not be completely covered, because sp^2 C–H sites, which are susceptible to Friedel–Crafts acylation, are less than a few percent. To be full explanation for uniformity, we believe the defective sp^2 C–H sites as well as non-defective sp^2 C on the surface of CNT are susceptible to covalent attachment. It would not be pure electrophilic substitution reaction for the later case. If we speculate the possible mechanism, there may be addition–substitution reaction beside electrophilic substitution reaction. To explain the possible mechanism, we are currently under investigation of C_{60}, which has only sp^2 C without defects.

3.7. Compression molding

The VGCNF-*g*-*m*PEK nanocomposites were easily compression-molded (Fig. 8). Thus, VGCNF-*g*-*m*PEK samples were heated under pressure in a Carver Laboratory Press at 150–160 °C for 10 min to afford 6×70 mm (1.2–1.4 mm thickness) sample bars (Fig. 8). Thus, it is expected this family of thermoplastic nanocomposites could be easily processed and fabricated with the conventional molding techniques, and with this value-added feature, their commercialization potential should be greatly enhanced.

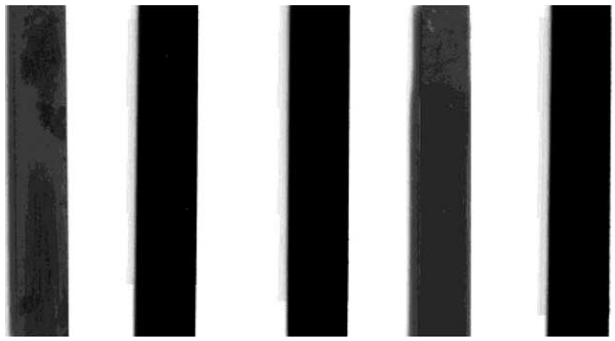

Fig. 8. Compression-molded parts of VGCNF-*g*-*m*PEK.

4. Conclusions

Polyphosphoric acid (PPA) with optimized P_2O_5 content as an electrophilic-substitution-reaction medium is indeed benign and effective for the covalent attachment of polyetherketones onto the surface of the electron-deficient MWNT and VGCNF. Furthermore, on the basis of all supportive evidences, this work provides one of the most efficient methods to directly and uniformly grafting the surfaces of carbon nanotubes (CNT) and nanofibers (CNF) without or minimum damages. More importantly, the fact that the isolated nanocomposites were easily processed and fabricated with the conventional molding techniques and 5 wt% nanocomposite/PPA dopes could be wet-spun into a single fiber simply by the force of gravity. With this value-added feature, their commercialization potential should be greatly enhanced. This work is envisioned that one of the best tools in the field of chemical modification of carbon nanomaterials for application-specific purpose without concerning interfacial interaction between carbon nanomaterial and matrix, which often considered in physical dispersion of carbon nanomaterial into matrix.

Acknowledgements

We are grateful to Jeong Hee Lee and Woo Jin Choi of Chungbuk National University for conducting SEM and Thermal Analysis. We thank US Air Force Office of Scientific Research, Asian Office of Aerospace Research and Development (AFOSR-AOARD054027) and Korea Research Foundation (R05-2004-000-10215-0) for their financial supports of this research.

References

[1] Dresselhaus MS, Dresselhaus G, Eklund PC. Science of fullerenes and carbon nanotubes. San Diego, CA: Academic Press; 1996.
[2] Maruyama B, Khairul Alam M. Thermal conductivity of carbon foams. SAMPE J 2003;38(3):59–60.
[3] Hu J, Odom TW, Lieber CM. Chemistry and physics in one dimension: synthesis and properties of nanowires and nanotubes. Acc Chem Res 1999;32(5):435–45.

[4] Journet C, Maser WK, Bernier P, Loiseau A, Lamy de la Chappelle C, Lefrant S, et al. Large-scale production of single-walled carbon nanotubes by the electric-arc technique. Nature 1997;388:756–8.
[5] Andrews R, Jacques D, Rao AM, Rantell T, Derbyshire F, Chen Y, et al. Nanotube composite carbon fibers. Appl Phys Lett 1999;75(9):1329–31.
[6] Qian D, Dickey EC, Andrews R, Rantell T. Load transfer and deformation mechanisms in carbon nanotube-polystyrene composites. Appl Phys Lett 2000;76(20):2868–70.
[7] Shaffer MSP, Windle AH. Fabrication and characterization of carbon nanotube/poly(vinyl alcohol) composites. Adv Mater 1999;11(11): 937–41.
[8] Zin L, Bower C, Zhou O. Alignment of carbon nanotubes in a polymer matrix by mechanical stretching. Appl Phys Lett 1998;73(9):1197–9.
[9] Haggenmueller R, Gommans HH, Rinzler AG, Fischer JE, Winey KI. Aligned single-wall carbon nanotubes in composites by melt processing methods. Chem Phys Lett 2000;330(3–4):219–25.
[10] Chen GZ, Shaffer MSP, Coleby D, Dixon D, Zhou W, Fray DJ, et al. Carbon nanotube and polypyrrole composites: coating and doping. Adv Mater 2000;12(7):522–6.
[11] Sandler J, Shaffer MSP, Prasse T, Bauhofer W, Schulte K, Windle AH. Development of a dispersion process for carbon nanotubes in an epoxy matrix and the resulting electrical properties. Polymer 1999;40(21): 5967–71.
[12] Part C, Ounaies Z, Watson KA, Crooks RE, Smith Jr J, Lowther SE, et al. Dispersion of single wall carbon nanotubes by in situ polymerization under sonication. Chem Phys Lett 2002;364(3-4):303–8.
[13] Sun Y-P, Fu K, Lin Y, Huang W. Functionalized carbon nanotubes: properties and applications. Acc Chem Res 2002;35(12):1096–104.
[14] Mitchell CA, Bahr JL, Arepalli S, Tour JM, Krishnamoorti R. Dispersion of functionalized carbon nanotubes in polystyrene. Macromolecules 2002; 35(23):8825–30.
[15] Monthioux M, Smith BW, Burteaux B, Claye A, Fischer JE, Luzzi DE. Sensitivity of single-wall carbon nanotubes to chemical processing: an electron microscopy investigation. Carbon 2001;39(8):1251–72.
[16] Zhang T, Shi Z, Gu Z, Iijima S. Structure modification of single-wall carbon nanotubes. Carbon 2000;38(15):2055–9.
[17] Heller DA, Barone PW, Strano MS. Sonication-induced changes in chiral distribution: a complication in the use of single-walled carbon nanotube fluorescence for determining species distribution. Carbon 2005;43(3): 651–3.
[18] Shaffer MSP, Fan X, Windle AH. Dispersion and packing of carbon nanotubes. Carbon 1998;36(11):1603–12.
[19] Cai L, Bahr JL, Yao Y, Tour JM. Ozonation of single-walled carbon nanotubes and their assemblies on rigid self-assembled monolayers. Chem Mater 2002;14(10):4235–41.
[20] Mickelson ET, Huffman CB, Rinzler AG, Smalley RE, Hauge RH, Margrave JL. Fluorination of single-wall carbon nanotubes. Chem Phys Lett 1998;296(1–2):188–94.
[21] Bahr JL, Yang J, Kosynkin DV, Bronikowski MJ, Smalley RE, Tour JM. Functionalization of carbon nanotubes by electrochemical reduction of aryl diazonium salts: a bucky paper electrode. J Am Chem Soc 2001; 123(27):6536–42.
[22] Bahr JL, Tour JM. Highly functionalized carbon nanotubes using in situ generated diazonium compounds. Chem Mater 2001;13(11):3823–4.
[23] Ge JJ, Zhang D, Li Q, Hou H, Graham MJ, Dai L, et al. Multiwalled carbon nanotubes with chemically grafted polyetherimides. J Am Chem Soc 2005;127(28):9984–5.
[24] Baek J-B, Tan L-S. Improved syntheses of poly(oxy-1,3-phenylenecarbonyl-1,4-phenylene) and related poly(ether-ketones) using polyphosphoric acid/P_2O_5 as polymerization medium. Polymer 2003;44(15): 4135–47.
[25] Baek J-B, Lyons CB, Tan LS. Covalent modification of vapour-grown carbon nanofibers via direct Friedel–Crafts acylation in polyphosphoric acid. J Mater Chem 2004;14(13):2052–6.
[26] Baek J-B, Lyons CB, Tan L-S. Grafting of vapor-grown carbon nanofibers via in situ polycondensation of 3-phenoxybenzoic acid in poly(phosphoric acid). Macromolecules 2004;37(22):8278–85.
[27] Baek J-B, Park SY, Price GE, Lyons CB, Tan L-S. Unusual thermal relaxation of viscosity-and-shear-induced strain in poly(ether-ketones) synthesized in highly viscous polyphosphoric acid/P_2O_5 medium. Polymer 2005;46(5):1543–52.
[28] http://www.iljinnanotech.co.kr.
[29] http://www.apsci.com.
[30] Ebbesen TW, Takada T. Topological and sp^3 defect structures in nanotubes. Carbon 1995;33(7):973–8.
[31] Meunier V, Lambin Ph. Scanning tunneling microscopy and spectroscopy of topological defects in carbon nanotubes. Carbon 2000;38(11–12): 1729–33.
[32] Qian W, Liu T, Wei F, Wang Z, Luo G, Yu H, et al. The evaluation of the gross defects of carbon nanotubes in a continuous CVD process. Carbon 2003;41(13):2613–7.
[33] Shimada T, Yanase H, Morishita K, Hayashi J, Chiba T. Points of onset of gasification in a multi-walled carbon nanotube having an imperfect structure. Carbon 2004;42(8–9):1635–9.
[34] Carneiro OS, Covas JA, Bernardo CA, Calderia G, Hattum FWJV, Ting JM, et al. Production and assessment of polycarbonate composites reinforced with vapour-grown carbon fibres. Compos Sci Technol 1998; 58(3–4):401–7.
[35] Liu M, Yang Y, Zhu T, Liu Z. Chemical modification of single-walled carbon nanotubes with peroxytrifluoroacetic acid. Carbon 2005;43(7): 1470–8.
[36] Digital photograph of MWNT-*g*-mPEK nanocomposite/PPA dope.
[37] Digital photograph of VGCNF-*g*-mPEK nanocomposite/PPA dope.
[38] Digital photograph of MWNT-*g*-pPEK nanocomposite/PPA dope.
[39] Digital photograph of VGCNF-*g*-pPEK nanocomposite/PPA dope.
[40] Movie for fiber spinning of MWNT-*g*-pPEK into distilled waters.
[41] Movie for fiber spinning of VGCNF-*g*-pPEK into distilled waters.
[42] [Melt spinning of VGCNF/thermoplastic nanocomposites have been reported: (a) polypropylene] Kumar S, Doshi H, Srinivasarao M, Park JO, Schiraldi DA. Fibers from polypropylene/nano carbon fiber composites. Polymer 2002;43(5):1701–3.
[43] [PMMA (10 wt%)] Zeng J, Saltysiak B, Johnson WS, Schiraldi DA, Kumar S. Processing and properties of poly(methyl methacrylate)/carbon nanofiber composites. Compos Part B, Eng 2004;35(3):245–9.
[44] [PET] Ma H, Zeng J, Realff ML, Kumar S, Schiraldi DA. Processing, structure, and properties of fibers from polyester/carbon nanofiber composites. Compos Sci Technol 2003;63(11):1617–28.
[45] [PEEK (10 wt%)] Sandler J, Windle AH, Werner P, Altstaedt V, Es MV, Shaffer MSP. Carbon-nanofibre-reinforced poly(ether ether ketone) fibres. J Mater Sci 2003;38(10):2135–41.
[46] [Solution spinning of VGCNF (10 wt%)/rigid-rod polymer] Uchida T, Dang TD, Min BG, Zhang X, Kumar S. Processing, structure, and properties of carbon nano fiber filled PBZT composite fiber. Compos Part B, Eng 2005;36(3):183–7.
[47] Kumar S, Dang TD, Arnold FE, Bhattacharyya AR, Min BG, Zhang X, et al. Processing, structure, and properties of carbon nano fiber filled PBZT composite fiber. Macromolecules 2002;35(24):9039–43.
[48] Lee H-J, Oh S-J, Choi J-Y, Kim JW, Han J, Tan L-S, et al. In situ synthesis of polyethyleneterephthalate in ethylene glycol containing terephthalic acid and functionalized multi-walled carbon nanotubes as an approach to MWNT/PET nanocomposites. Chem Mater 2005;17(20):5057–64.